Electronic Supporting Information

Endosome-escaping micelle complexes dually equipped with cell-penetrating and endosome-disrupting peptides for efficient DNA delivery into intact plants

Takaaki Miyamoto[†], *Kousuke Tsuchiya*[‡]*, *Keiji Numata*[†,‡]*

†Biomacromolecules Research Team, RIKEN Center for Sustainable Resource Science, 2-1 Hirosawa, Wako-shi, Saitama 351-0198, Japan

‡Department of Material Chemistry, Graduate School of Engineering, Kyoto University, Kyoto-Daigaku-Katsura, Nishikyo-ku, Kyoto 615-8510, Japan.

Contents

Supplementary methods

RP-HPLC analyses. We performed RP-HPLC analyses of the peptide-modified micelles as previously described (*Biomacromolecules* **2019**, 20, 653–661) with minor modifications. Specifically, the RP-HPLC system consisted of an auto sampler (AS-2055, JASCO, Tokyo, Japan), a gradient pump (PU2089, JASCO), a column oven (CO-4060, JASCO), and a C18 column (YMC-Triart C18, particle size 5 μm, 150 × 4.6 mm i.d., YMC, Kyoto, Japan). Each micelle solution prepared for the DLS measurements (800 μL, [pDNA] = 25 μg/mL, [MAL-TEG-$(KH)_{14}$] = 5 μM) was lyophilized and then dissolved in aqueous solution (100 μL) containing Boc-Pro-OH (2 mg/mL, an internal standard) and tris(2-carboxyethyl)phosphine hydrochloride solutions (50 mM, a reducing agent). The solution was incubated for 5 min to reduce a disulfide bond between the peptides. Then, the solution (100 μL) was injected into the RP-HPLC system with the mobile phase composed of Milli-Q water (eluent A), acetonitrile (eluent B), and 1% (v/v) TFA aqueous solution (eluent C). We used the following linear gradient conditions at a flow rate of 1 mL/min: Tat-MC, (A = 82%, B = 8%, C = 10 %) → (A = 67%, B = 23%, C = 10 %), 30 min; BP100-MC, KAibA-MC, KAibA/EED4-MC, and KAibA/LAH4-L1-MC, (A = 80%, B = 10%, C = 10 %) → (A = 20%, B = 70%, C = 10 %), 40 min; KAibA/GALA-MC, (A = 80%, B = 10%, C = 10 %) → (A = 0%, B = 100%, C = 10 %), 30 min. The column temperature was kept at 25 °C and elution of the various compounds was monitored by UV absorbance at 210 nm. Peak areas and retention times of eluting compounds were determined by chromatography software (ChromNAV, JASCO, Tokyo, Japan). Unreacted CPPs or EDPs were quantified from the peak area corrected by that of Boc-Pro-OH on the basis of a calibration curve, which was obtained by plotting the peak area of the peptide against the concentration. The conversion rate of MAL-TEG-$(KH)_{14}$ was estimated from the amount of unreacted peptide.

Supplementary figures and table

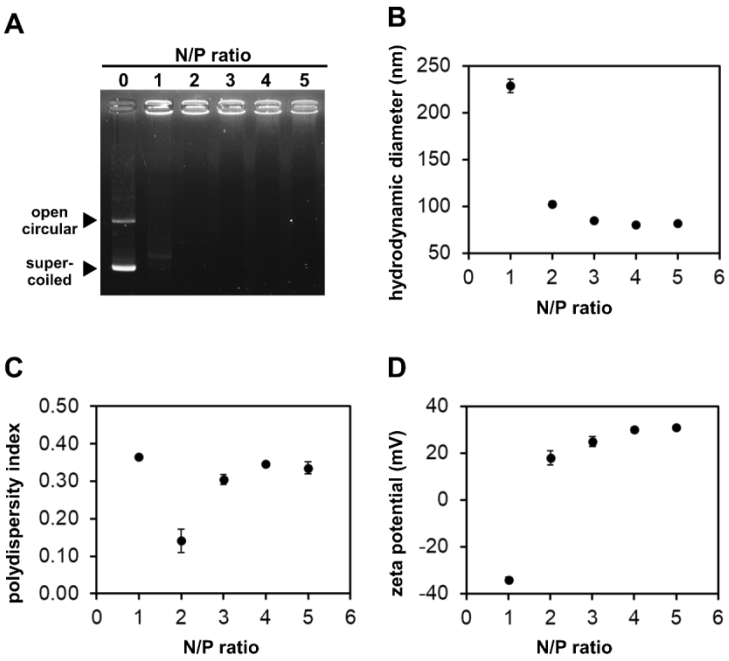

Fig. S1. Characterization of the MAL-TEG-$(KH)_{14}$/pDNA micelles at various N/P ratios. (A) Electrophoretic mobility shift assays of the naked pDNA (N/P = 0) and the micelles (N/P = 1–5). (B) Hydrodynamic diameters and (C) PDI values of the micelles (N/P = 1–5) obtained from the DLS measurements. Error bars represent standard errors (n = 3). (D) Zeta potentials of the micelles (N/P = 1–5). Error bars represent standard errors (n = 3).

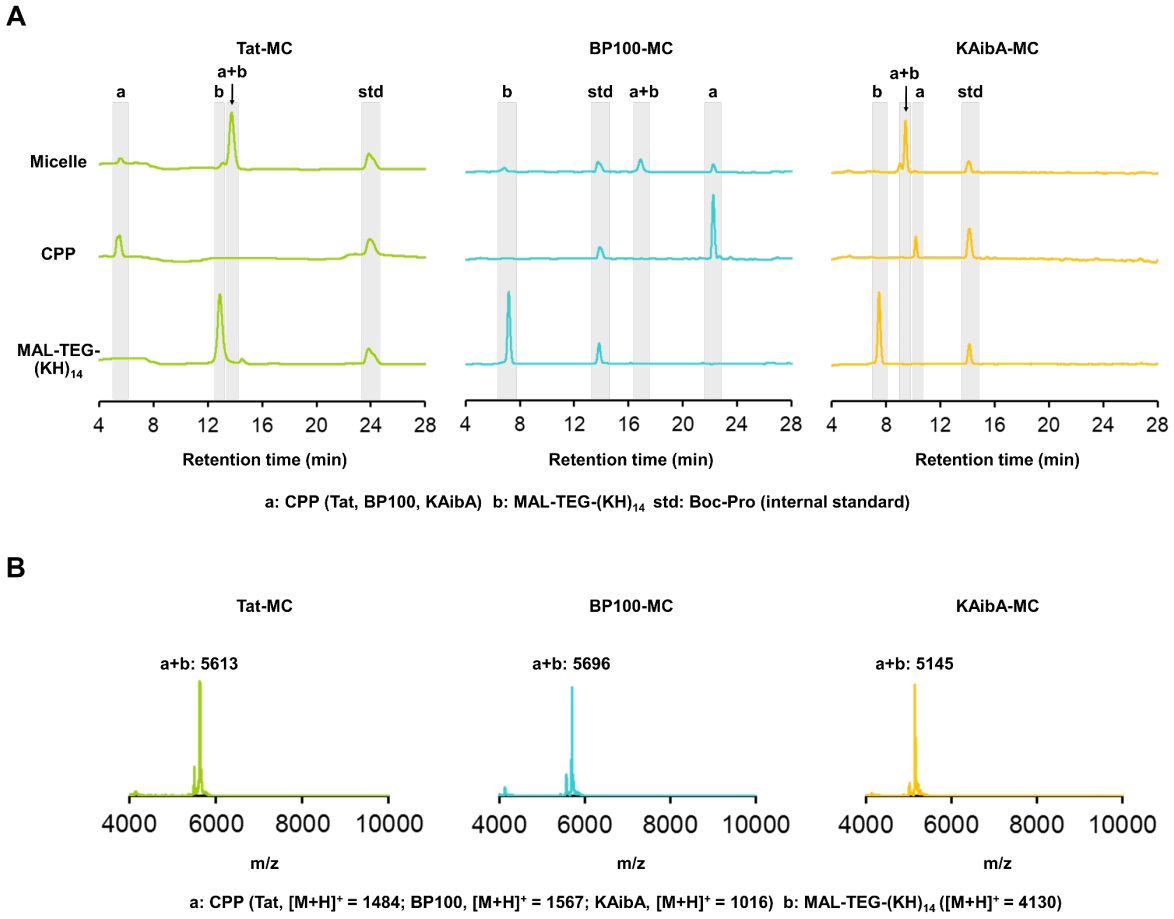

Fig. S2. RP-HPLC and MALDI-TOF MS analyses for the CPP-modified micelles. (A) RP-HPLC chromatograms of the CPP-modified micelles (Tat-MC, BP100-MC, or KAibA-MC), CPP, and MAL-TEG-$(KH)_{14}$. (B) MALDI-TOF MS spectra of the fraction "a+b" obtained from the RP-HPLC analysis shown in (A). The observed molecular weight of the fraction corresponded to the calculated molecular weight of the CPP-MAL-TEG-$(KH)_{14}$ conjugate, indicating that the micelle was successfully modified with the CPP.

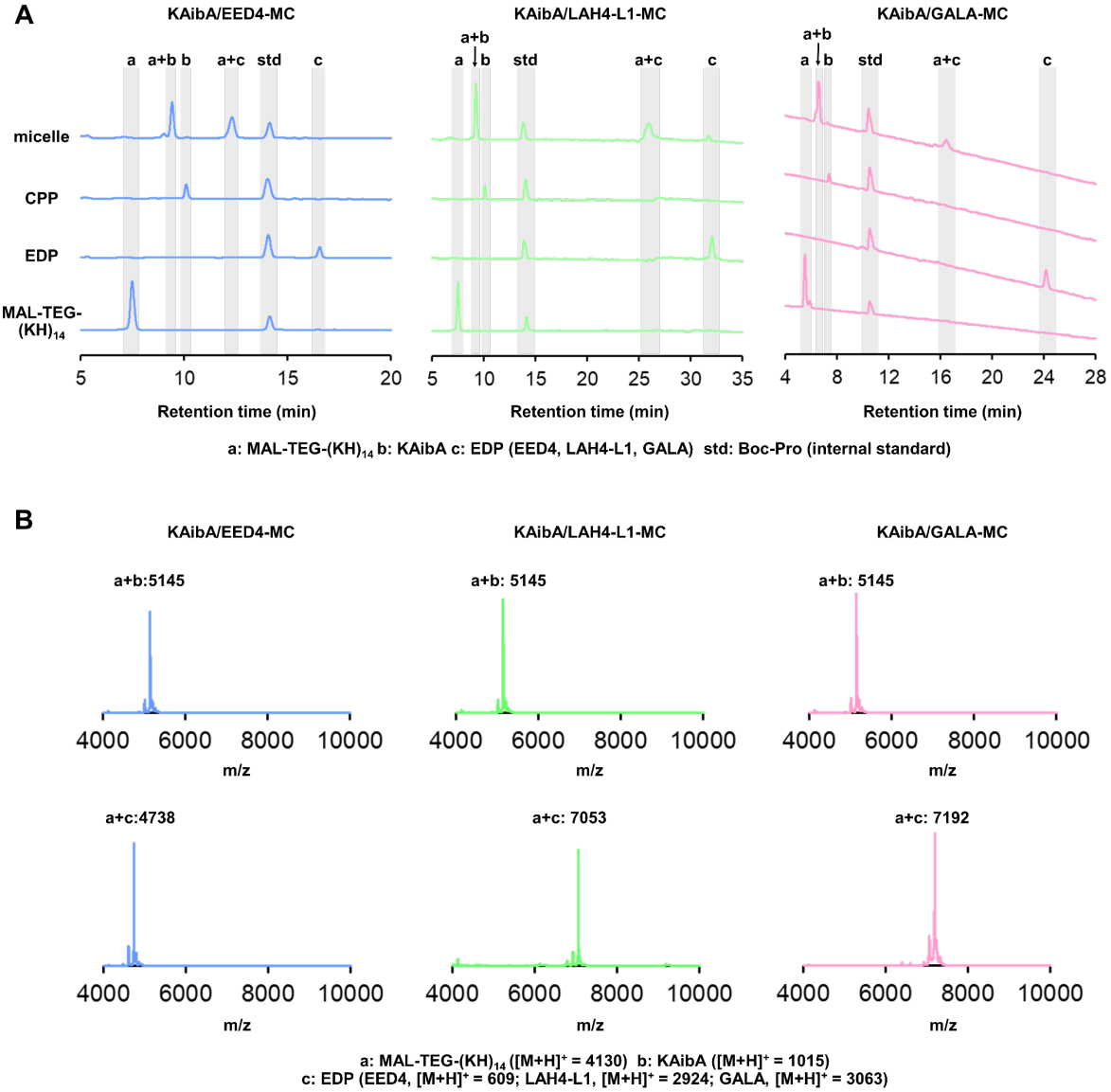

Fig. S3. RP-HPLC and MALDI-TOF MS analyses for the CPP/EDP-modified micelles. (A) RP-HPLC chromatograms of the CPP/EDP-modified micelles (KAibA/EED4-MC, KAibA/LAH4-L1-MC, or KAibA/GALA-MC), CPP, EDP, and MAL-TEG-$(KH)_{14}$. (B) MALDI-TOF MS spectra of the fractions "a+b" and "a+c" obtained from the RP-HPLC analysis shown in (A). The observed molecular weights of the fractions "a+b" and "a+c" corresponded to the calculated molecular weights of the CPP- and EDP-MAL-TEG-$(KH)_{14}$ conjugates, respectively. These results indicated that the micelle was concomitantly modified with the CPP and EDP.

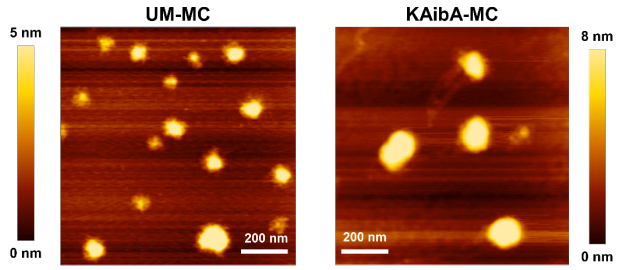

Fig. S4. AFM observations of the unmodified (UM-MC) and KAibA-modified (KAibA-MC) micelles. Color bars represent the height of the micelle.

A

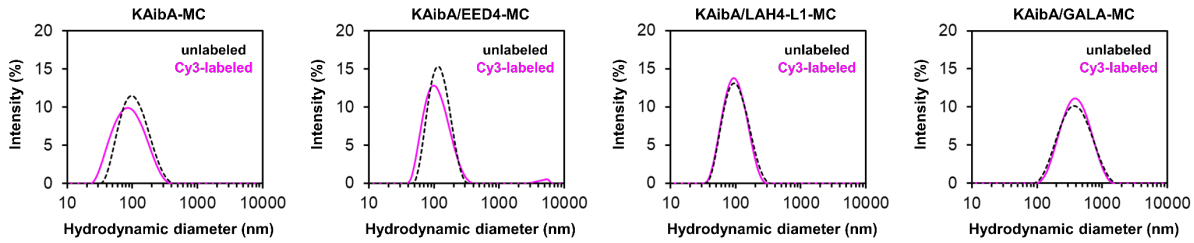

B

	unlabeled		Cy3-labeled		Cy3-labeled (with wortmannin)		Cy3-labeled (with concanamycin A)	
	Z-Average (nm)	PDI	Z-Average (nm)	PDI	Z-Average (nm)	PDI	Z-Average (nm)	PDI
KAibA-MC	94 ± 3	0.15 ± 0.02	81 ± 1	0.22 ± 0.01	80 ± 1	0.23 ± 0.01	n.d.	n.d.
KAibA/EED4-MC	110 ± 2	0.10 ± 0.02	101 ± 2	0.20 ± 0.00	107 ± 1	0.20 ± 0.01	103 ± 1	0.18 ± 0.01
KAibA/LAH4-L1-MC	94 ± 1	0.17 ± 0.03	90 ± 3	0.18 ± 0.01	95 ± 2	0.23 ± 0.01	90 ± 1	0.23 ± 0.00
KAibA/GALA-MC	331 ± 10	0.21 ± 0.02	387 ± 26	0.21 ± 0.04	366 ± 6	0.26 ± 0.02	n.d.	n.d.

Fig. S5. DLS measurements of the fluorescently labeled micelles in the absence and presence of wortmannin and concanamycin A. (A) Intensity size distributions of the unlabeled and fluorescently labeled micelles. (B) Z-average diameters and PDI of the unlabeled or the fluorescently labeled micelles in the absence or presence of wortmannin and concanamycin A. The diameters and PDI of fluorescently labeled KAibA and KAibA/GALA were not determined (n.d.) in the presence of concanamycin A.

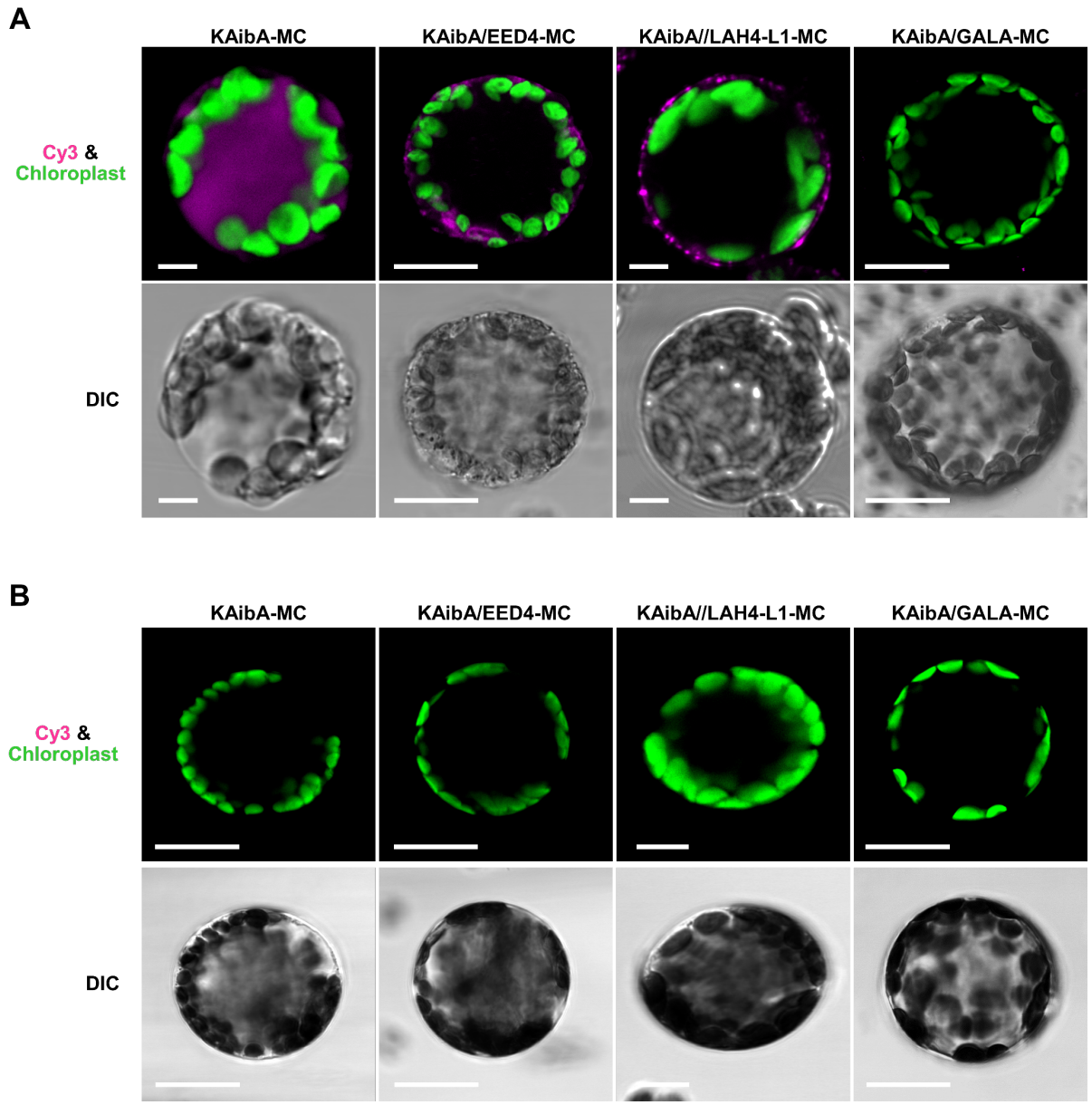

Fig. S6. CLSM observations of the fluorescently labeled micelles in protoplasts obtained from transfected *A. thaliana* cotyledons. CLSM images of the transfected cotyledons (A) without and (B) with wortmannin treatment. The pDNA and chloroplasts were visualized by the fluorescence signals of Cy3 (magenta) and chlorophyll (green), respectively, whereas protoplasts are displayed in the "DIC" images. Scale bars represent 5 μm.

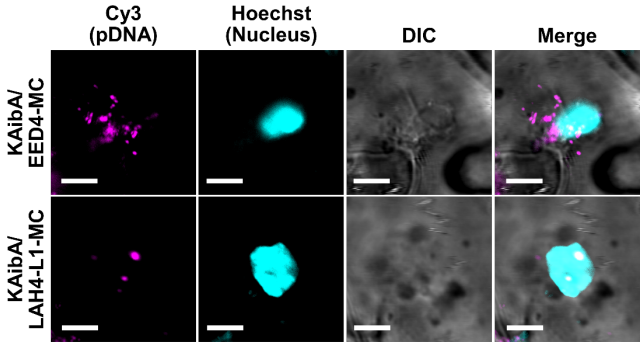

Fig. S7. CLSM observations to confirm the colocalization of the fluorescently labeled micelles and the Hoechst-stained nucleus in *A. thaliana* cotyledons 24 h post-infiltration. The pDNA (micelle) was visualized by Cy3 fluorescence, whereas the nuclei were detected by Hoechst fluorescence. The cells are displayed in DIC. The "Merge" images show the composites of the Cy3, Hoechst, and DIC images. Scale bars represent 5 μm.

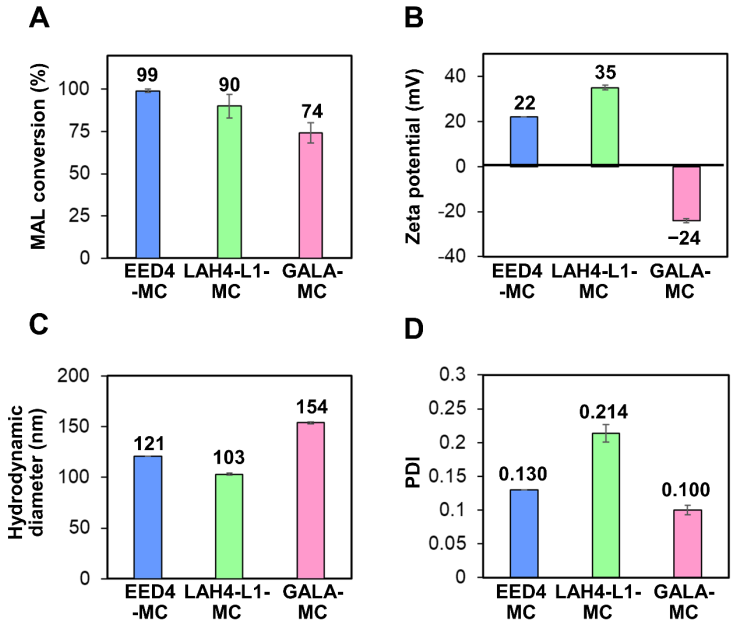

Fig. S8. Characterization of the EDP-modified micelles through RP-HPLC, zeta potential, and DLS analyses. (A) Conversion of maleimide groups in the EDP-modified micelles determined by RP-HPLC analysis. Data are represented as mean ± standard error values (n = 3). (B) Zeta potentials, (C) hydrodynamic diameters, and (D) PDI of the EDP-modified micelles obtained from zeta potential and DLS measurements. Data are represented as mean ± standard error values (n = 3).

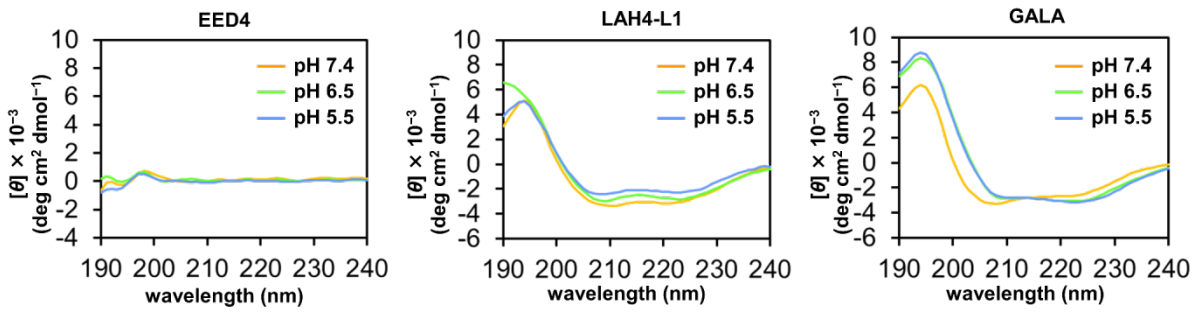

Fig. S9. CD measurements of the unconjugated EDPs at neutral and weakly acidic pH. CD spectra of the EED4, LAH4-L1, and GALA peptides were measured at pH 7.4, 6.5, and 5.5 in aqueous solution containing 5 mM HEPES (25 °C).

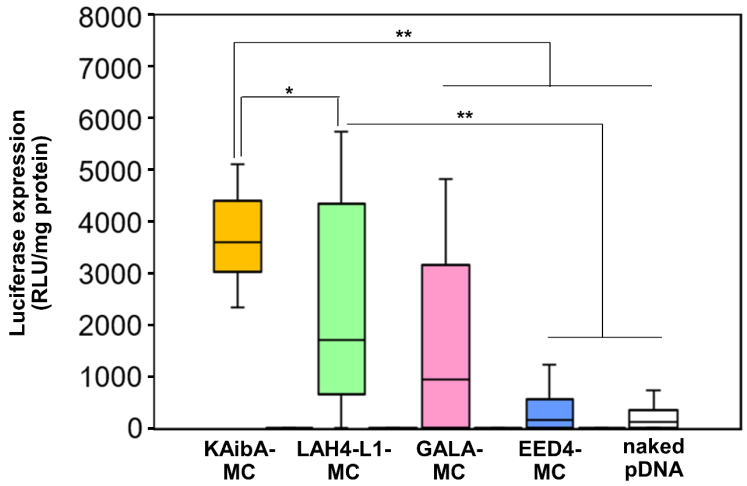

Fig. S10. Transfection efficiency of the EDP-modified micelles based on the luciferase expression level in *A. thaliana* seedlings. The data from 20 biologically independent samples for each system are represented in a box plot format: boxes represent the interquartile range; lines within the boxes represent the median values; and upper and lower whiskers represent the highest and lowest values, respectively. Statistical significance was set at $P < 0.05$ (*) and $P < 0.01$ (**) based on Mann-Whitney *U*-tests (n = 20).

Table S1. Physicochemical properties of the micelles prepared from GFP- or luciferase-coded pDNA. The Z-average diameters, PDI, and zeta potentials are represented as mean ± standard error values (n = 3).

	pDNA: *p*35S-Nluc-*t*NOs			pDNA: *p*35S-GFP-*t*NOs		
	Z-Average (nm)	**PDI**	**Zeta potential (mV)**	**Z-Average (nm)**	**PDI**	**Zeta potential (mV)**
KAibA-MC	94 ± 3	0.15 ± 0.02	27 ± 1	95 ± 1	0.17 ± 0.01	32 ± 1
KAibA/EED4-MC	110 ± 2	0.10 ± 0.02	24 ± 0	103 ± 1	0.17 ± 0.00	30 ± 1
KAibA/LAH4-L1-MC	94 ± 1	0.17 ± 0.03	25 ± 0	95 ± 1	0.20 ± 0.01	33 ± 1
KAibA/GALA-MC	331 ± 10	0.21 ± 0.02	7 ± 0	263 ± 7	0.29 ± 0.04	10 ± 0